

# NOVEL TRANSPORT SIMULATION OF VERTICALLY-GROWN MOSFETs BY CELLULAR AUTOMATON METHOD

A. Rein, G. Zandler, M. Saraniti, P. Lugli<sup>+</sup>, and P. Vogl

*Physik Department and Walter Schottky Institut  
TU München, D-85747 Garching, FRG*

## Abstract

We present a theoretical study of vertically-grown Silicon ultra-short FET's. For a gate length of 50nm a transconductance of at least 1000 mS/mm and a maximum transit time frequency of 200 GHz are predicted. A sensitive influence of the doping profile on short channel effects is demonstrated. Our simulations are based on a new implementation of the Cellular Automata method, which provides a significant suppression of statistical errors. To take advantage of the high speed of the Cellular Automaton a fast multigrid-solver for the Poisson equation has been developed.

## Introduction

The physical effects involved in scaled down sub- $\mu\text{m}$  devices require accurate simulation tools (1-3). The Monte Carlo (MC) technique (4,5) is at present the most valuable approach to account for hot carrier effects and non-local transport phenomena typical for such devices. Recently, a cellular automaton (CA) approach (6) has been developed as an efficient and discrete variant of the MC. In its first implementation, the CA was proven to give comparable results to the MC for a variety of devices (6-8). In this paper we introduce new developments in the CA method that allow more precise control and efficient suppression of statistical errors. The central point is to replace the probabilistic treatment of the electric field used in (6) by a deterministic hopping of the particles in a three dimensional and periodic k-space. Furthermore, in order to take advantage of the high intrinsic speed of the CA, we have developed a fast and efficient Poisson solver for general device geometries based on the multigrid method. The new CA device simulator has been applied to study planar doped barrier field effect transistors (PDBFET) with a gate length down to 50 nm. The results show the high speed capabilities of this vertical device and indicate possible strategies of further optimizations.

## New developments in the Cellular Automaton method

A cellular automaton is a discrete dynamical system which evolves in discrete time steps (9). It is defined at the nodes of a lattice, each site of which is characterized by a finite number of Boolean states. In the context of transport theory, these Boolean states are considered as representing fictitious "particles" carrying discrete values of momentum,

energy, and other quantum numbers. In each time step, a set of transition rules updates these states synchronously on all lattice sites. Such rules are local in the sense that the change of a Boolean state in one time step only depends on the states on the same and the neighboring lattice nodes. This locality of the dynamical rules allows an efficient and flexible handling of complex geometries and lattice topologies.

Recently (6), the full Boltzmann equation (BE) has been transformed into a CA, where the kinetic terms of the BE are replaced by hopping probabilities in such a way that the equations of motion are fulfilled on the average for an ensemble of quasi particles. In an explicit procedure, the drift term of the BE has been transformed into probabilistic field scattering rates. This corresponds to a substitution of the free flight by a random walk. For very high electric fields, this procedure leads to artificial diffusion in k-space. Associated with this diffusion is an enhancement of the kinetic energy, the entropy and the diffusivity. For a *periodic* momentum discretization, this statistical error can be estimated analytically as follows. The CA-scattering probability to nearest neighbor sites due to the electric field  $E(R)$  at lattice site  $R$  is given by (6)  $P_E = e\Delta t E(R)/(\hbar\Delta k)$ , where  $\Delta k$  is the lattice constant of the periodic k-space lattice,  $\Delta t$  the timestep,  $e$  the elementary charge and  $\hbar$  the Plank constant. After a timestep, a particle moves to one of the nearest neighbor cells with probability  $P_E$  while it remains in the same cell with probability  $1-P_E$ . The k-space diffusion associated with this random walk is given by  $D_{art} = \Delta k^2 P_E(1 - P_E)/(2\Delta t)$ . In principle, this artificial diffusion can be reduced by a sufficiently small lattice constant  $\Delta k$ , however this becomes impractical in a three dimensional momentum space.

We now show that it is possible to transform the drift term of the BE into a new *deterministic* hopping rule of the CA that completely suppresses this statistical error. The main point is to replace the probabilistic scattering rate by a discrete free flight. We derive this scattering rule by calculating the number of time steps  $N$  a particle needs to change its momentum by an amount equal to the lattice constant  $\Delta k$  in k-space. To illustrate the procedure, we restrict ourselves to one dimension; the generalization to more dimensions is straightforward. Integration of the semiclassical equation of motion  $\dot{k} = eE(r(t))/\hbar$  gives

## 14.2.1

$$\Delta k = k(t + \tau) - k(t) = \frac{e}{h} \int_t^{t+\tau} dt' E(r(t')) . \quad (1)$$

Let us denote the initial time by  $t = t_0$ , and assume that  $\tau = N\Delta t = t_N - t_0$  and set the real space position at time  $t_i$  equal to lattice vector  $R(t_i)$ . The discrete version of Eq. (1) reads

$$\Delta k = \sum_{i=0}^N \Delta t \frac{e}{h} E(R(t_i)) , \quad (2)$$

which is a condition for  $N$  and yields a deterministic scattering rule for the electric field: A particle remains in its  $k$ -cell for  $N$  time steps and hops subsequently into its nearest neighbor cell. Consequently, this procedure confines the statistical error to one  $k$ -cell. With this procedure, only of the order of  $10^3$  3-D  $k$ -cells are required for a nonparabolic band structure up to 2 eV. The lattice we have chosen is a hexagonal close-packed structure where each cell has twelve nearest neighbors. The restriction to nearest neighbors transforms the drift-term of the BE into a *local* interaction on momentum cells, in complete analogy to the treatment of the real-space diffusion-term of the BE (6).

Importantly, we found that the new implementation of the CA does not require more computer time per iteration than our earlier two-dimensional implementation (6) even though it is significantly more accurate.

### Multigrid-solver for the Poisson equation

Due to the intrinsic high speed of the CA algorithm, an efficient self consistent simulation requires a comparably fast Poisson solver. This is not achievable by applying standard Successive Overrelaxation (SOR) (10) techniques. In fact, an SOR-based solver takes about 90 percent of the overall simulation time. We have therefore developed a novel approach based on an iterative multigrid (MG) method.

The basic idea of the SOR, and of any other stationary iterative method, is to approach the “correct” solution by successive iterations, starting from an initial approximation. At each iteration, the algebraic error, that is the difference between the current approximation and the exact solution, is reduced with respect to the previous iteration. The major drawback of the SOR is to reduce the error efficiently only on a typical length scale determined by the discretization. A Fourier analysis of the error reduction shows (11,12) that only the high frequency Fourier components of the error are strongly reduced, since they match the range of the discretized operator, whereas the amplitude of the low frequency components decays very slowly. This problem is solved in the MG approach by the application of an iterative method on a succession of coarser and coarser grids, through

which the error is “restricted” via weighted averages. Since on each grid the resolution of the operator is different due to the different grid spacing, all the Fourier components of the error are reduced with the same efficiency, giving a dramatic speedup with respect to single-grid iterative methods. From the above description it is clear that a crucial component of the MG Poisson solver is the iterative method used to relax (or *smooth*) the error. In the realistic case of an inhomogeneous grid with rectangular cells, we found that the linewise relaxation scheme (10), which reduces the error simultaneously on all the points of one grid line, exhibits better performance than the pointwise relaxation.

The speed improvement obtained by using the MG Poisson solver is more than one order of magnitude with respect to the SOR, even with unfavorable boundary conditions (13). This speed up makes the solution of PE in the simulation as fast as a CA step, thus removing the bottleneck due to the unbalanced ratio between CA and SOR. Tests made with typical device structures (MOSFET, HEMT, MESFET) and various boundary conditions (13) have demonstrated the robustness of our MG Poisson solver.

### Transport simulations of PDBFETs

The new CA described above has been applied to a Si-PDBFET (14). This transistor is a vertically grown variant of a Si-MOSFET that contains a  $p^+$   $\delta$ -layer in the intrinsic region between the contacts instead of a homogeneous  $p$ -buffer (Fig. 1 (a)). Typical gate lengths that can be achieved

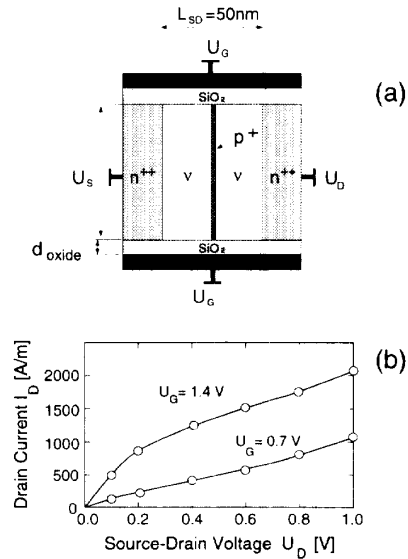


FIG 1. (a) Geometry of a vertically grown 50 nm planar-doped barrier FET. The  $n^{++}$  doping concentration is  $10^{19} \text{cm}^{-3}$ , the  $\delta$ -buffer has a width of 5 nm and a maximum doping concentration of  $5 \times 10^{18} \text{cm}^{-3}$ . (b) Typical calculated drain-current characteristics for two gate voltages  $U_G=0.7$  V and 1.4 V.

## 14.2.2

are 50 nm or smaller. In the present simulations, we used a gate length of 50 nm and a thickness of the  $p^+$ -layer of 5 nm. We found that a doping concentration of the  $\delta$ -layer up to  $5 \times 10^{18} \text{cm}^{-3}$  guarantees that no free holes are present to deteriorate the device performance. Fig. 1 (b) depicts the computed drain characteristics of a PDBFET. The results show typical short-channel effects. In particular, the drain current does not saturate at high drain voltages. This is due to the fact that the drain current cannot be efficiently controlled by the gate. In addition, velocity overshoot already appears at low drain voltages, as shown for a bias point at  $U_D=0.2$  V and  $U_G=1.4$  V in Fig. 2 (b). At this bias point, transport occurs only at the Si/SiO<sub>2</sub> interface. The corresponding longitudinal electric field is shown by the full line in Fig 2 (a). In the bulk diode the electric field (dashed line in Fig 2 (a)) constrains the electrons to the  $n^{++}$  regions. Contrary to the continuously increasing field in the inversion channel of an ultra-short MOSFET, the channel field in the two intrinsic regions is nearly homogeneous and has a magnitude of approximately 20 kV/cm. In the narrow p-buffer, on the other hand, there is a strongly inhomogeneous field that causes velocity overshoot of the carriers. For higher drain voltages, the channel field maintains its high value from the p-layer through the complete i-zone up to the  $n^{++}$  region of the drain contact. This leads to velocity overshoot nearly over the total channel length (Fig. 2 (b)). At the same time, the bulk field on the source side of the p-layer decreases, thus leading to parasitic conduction through the bulk diode. In contrast to short channel MOSFETs, the gate contacts are

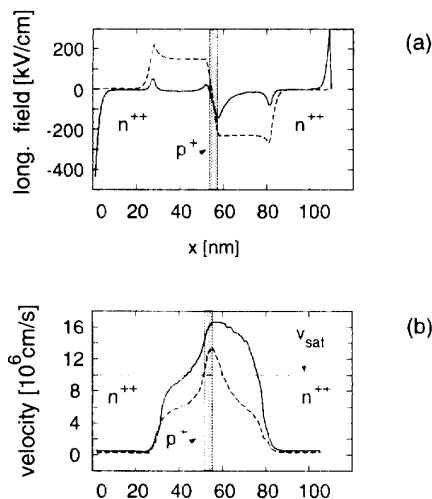


FIG 2. (a) Longitudinal electric field for a bias point at  $U_G=1.4$  V and  $U_D=0.2$  V (other parameters as in Fig. 1). The field in the inversion channel (full line) is approximately constant in the intrinsic regions and exhibits a sharp maximum in the p-layer. The field in the bulk diode (dashed line) confines the electrons to the  $n^{++}$  regions. (b) Vertically averaged drift velocity of the electrons at two bias points:  $U_D=0.2$  (dashed line) and  $U_D=0.6$  (full line).  $v_{\text{sat}}$  denotes the saturation velocity.

extended over the highly doped regions. This leads to a considerable reduction of impact ionization due to the lower junction field. The transient time frequency predicted by our simulations is not penalized by the enhanced gate capacitance, reaching values as high as 200 GHz, mainly thanks to the very high transconductance of at least 1000 mS/mm.

We found, that the high speed capability of the PDBFET can be optimized by shifting the  $\delta$ -layer towards the source contact. In this case a strong electric field is found already on the source side of the channel, thus sustaining the velocity overshoot over the whole channel. This leads to an enhanced current for low drain voltages compared to PDBFET's with a centered p-buffer (Fig. 3). On the other hand, the built-in potential due to the shifted  $\delta$ -layer is less influenced by the drain voltage. This improves the saturation of the drain current significantly and enhances the punch-through voltage of the barrier diode shown in Fig. 3. Our simulations predict

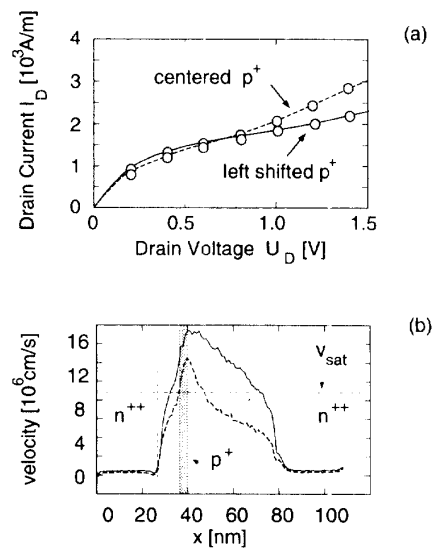


FIG 3. (a) Drain characteristics calculated for two PDBFETs using a left shifted (full line) and a centered p-layer (dashed line). (b) Vertically averaged drift velocity of the electrons in the channel of the PDBFET with left shifted p-layer. At low voltages (dashed line) higher velocities of the carrier are detected at the source side of the channel leading to higher drain currents than in the centered case.

a minimum output conductance when the p-layer is located 8 nm apart from the highly doped source region (Fig. 4). For smaller distances an increase in the channel conductance has been detected due to a decrease of the built-in potential of the p-layer.

## 14.2.3

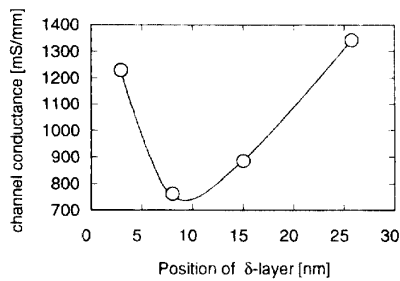


FIG 4. Optimization of the PDBEFT: The channel conductance is plotted as a function of the  $p^+$ -layer position apart from the highly doped source region. Our calculation predict a minimum channel conductance for a  $p$ -layer located at 8 nm.

Goßner et al. (14) measured a drain current about two orders of magnitude lower than the one obtained by the simulation. We believe that this difference is due to the poor quality of the Si/SiO<sub>2</sub> interface (14), which causes a large numbers of surface traps to be present and to reduce the current capabilities of the transistor. With respect to more standard MOSFET structures, the gate insulator was formed by thermal oxidation of vertically-etched lateral Si surfaces, a process which is at the moment not very well controlled. Taking into account a surface charge of  $5 \times 10^{13} \text{ cm}^{-3}$  we are indeed able to reduce the calculated current to the low level measured in the fabricated device.

### Conclusion

We have presented new improvements in the cellular automaton approach for high field transport in semiconductors. A deterministic rule for the electric field in the CA leads to a significant reduction of the statistical errors in a fully three dimensional  $k$ -space discretization. We coupled the CA to a fast Multigrid Poisson Solver, which is at least one order of magnitude faster than traditional relaxation methods as SOR. We also demonstrated the high speed capability of Si-PDBFET's resulting in a transconductance of 1000 mS/mm, a transit-time frequency of 200 GHz and no relevant influence of impact ionization compared to short channel MOSFETs.

The PDBFET can be optimized by a shifted  $\delta$ -layer towards the source contact.

\*Permanent address: Dipartimento di Ingegneria Elettronica, Università di Roma "Tor Vergata", I-00133 Rome, Italy

### References

1. S. Selberherr, "Analysis and Simulation of Semiconductor Devices", (Springer, Wien, 1984)
2. W. L. Engl, editor, "Process and Device Modeling" (Elsevier, Amsterdam, 1986)
3. K. Hess, J. P. Leburton, U. Ravaioli, "Computational Electronics" (Kluwer Academic, Norwell, MA, 1991)
4. M. Fischetti and S. E. Laux, "Monte Carlo analysis of electron transport in small semiconductor devices including band-structure and space-charge effects", *Phys. Rev. B* **38**, 9721 (1988)
5. C. Jacoboni and P. Lugli, "The Monte Carlo Method for Semiconductor Device Simulation", (Springer, Wien, 1989)
6. K. Kometer, G. Zandler and P. Vogl, "Lattice-gas cellular automaton method for semiclassical transport in semiconductors" *Phys. Rev. B* **46**, 1382 (1992)
7. G. Zandler, A. Di Carlo, K. Kometer, P. Lugli, P. Vogl and E. Gornik, "A comparison of Monte Carlo and cellular automaton approaches for semiconductor device simulation", *IEEE Electron Dev. Letters* **14**, 77 (1993)
8. G. Zandler, A. Rein, M. Saraniti, P. Vogl, P. Lugli, "Can cellular automata methods compete with Monte Carlo semiconductor device simulations?", *Proceedings of the 23rd ESSDERC* (J. Borel, P. Gentil, J.P. Noblanc, A. Nouailhat, M. Verdone, eds.), pp. 21-28, (Edition Frontiers, Gif-sur-Yvette Cedex, 1993)
9. P. Manneville, N. Boccara, G. Vichniac, "Cellular Automata and Modeling of Complex Physical Systems", *Proceedings in Physics* **46** (Springer, Heidelberg, 1989)
10. D. M. Young, "Iterative Solution of Large Linear Systems", Computer Science and Applied Mathematics, (Academic Press, New York, 1971)
11. A. Brandt, "Multigrid techniques: 1984 guide with applications to fluid dynamics," Monograph 85, Ges. für Mathematik u. Datenverarbeitung mbH Bonn, Postfach 1240, D-5205, St. Augustin 1, Germany, May 1984.
12. R. Kettler, "Analysis and comparison of relaxation schemes in robust multigrid and preconditioned conjugate gradient methods," in *Multigrid Methods; Proceedings of the Conference Held at Köln-Porz, November 23-27, 1981* (W. Hackbusch and U. Trottemberg, eds.), no. 960 in Lecture Notes in Mathematics, pp. 502-534, (Springer, Berlin, 1982)
13. M. Saraniti, A. Rein, G. Zandler, P. Vogl, and P. Lugli, "An efficient multigrid Poisson solver for Monte Carlo and cellular automaton device simulators," unpublished
14. H. Gossner, I. Eisele and L. Risch, "Realization of a vertical Si-MOSFET with a gate length of 50nm by molecular beam epitaxy", *Jap. Journal of Appl. Phys.*, **33**, pp. 2423-2428, (1994).